Hindawi
Advances in Materials Science and Engineering
Volume 2023, Article ID 2092339, 12 pages
https://doi.org/10.1155/2023/2092339

Research Article

Evaluation of Pure Titanium Welded Joints Produced by Underwater Friction Stir Welding

S. Meikeerthy,[1] N. Ethiraj,[1] Ibsa Neme ,[2] and Chandran Masi [2]

[1]*Department of Mechanical Engineering, Dr. M.G.R Educational and Research Institute, Maduravoyal, Chennai-600095, Tamilnadu, India*
[2]*Department of Biotechnology and Chemical Engineering, College of Biological and Chemical Engineering, Addis Ababa Science and Technology University, Addis Ababa, Ethiopia*

Correspondence should be addressed to Chandran Masi; chandran.chandran@aastu.edu.et

Received 29 July 2022; Revised 22 December 2022; Accepted 28 December 2022; Published 4 January 2023

Academic Editor: Baskaran Rangasamy

Underwater friction stir welding (UWFSW) is an advancement of conventional friction stir welding, which is performed in air. The need for welding underwater calls for more information to be explored in the welding of different materials. The aim of this research is to investigate the UWFSW of 2 mm titanium sheet joints for their tensile and microstructural properties and compare them with the results of friction stir welding (FSW) performed in air. Also, nondestructive tests, such as radiography and dye penetrant tests, were carried out to identify the occurrence of any weld defects. The rotational speed of the FSW tool and its travelling speed were considered process parameters, while other parameters like the tilt angle of the tool, shape of the tool pin, etc. were kept constant. The results show that the welded joints with higher strengths were achieved at a lower travelling speed of 140 mm/min at a rotational speed of 400 and 500 rpm in FSW and UWFSW, respectively. The mechanical properties such as yield strength, tensile strength, and hardness are improved in UWFSW when compared with conventional FSW due to the proper mixing of the metal and effective cooling due to the water environment. In underwater FSW, the improved YS and TS values are observed, which are 95.9% and 75.1% of the base metal values, respectively, when the tool rotational speed is 400 rpm and the travelling speed is 140 mm/min. However, the elongation % is much lower in both FSW and UWFSW when compared with the base metal. These results are supported by microstructure and nondestructive test outcomes.

1. Introduction

The increasing need for eco-friendly manufacturing processes has created a platform for researchers to explore newer materials and techniques. Friction stir welding (FSW) is one of the novel green metal joining processes in which there is no formation of fumes and gases that affect the environment and humans due to the nonusage of electrodes. FSW, a mature solid-state welding process involving temperature, mechanics of plastic deformation, metallurgy, and interactions has become a revolutionary welding process due to its energy efficiency, eco-friendliness, and ability to produce high-quality joints [1]. It is a promising joining technology for butt-joints of the long-distance butt or lapped joints of aircraft structures, whereas the high-speed and easily controllable laser beam welding process allows the joining of complex geometrical forms [2].

The heat energy generated by the friction between the rotating tool and the workpiece is utilized for welding by plasticizing the material, and joints are made in a solid-state condition [2–5]. The important process parameters used for welding are the rotational speed of the tool, the travelling speed of the tool, the tool pin dimension, the tool pin shape, and the axial force [6]. Some researchers believed that tool shoulder diameter, tool tilt angle, and tool material were critical for successful welding processes [7]. Apart from the welding of various similar materials, such as Al-, Mg, Cu-, Ti-alloys, and steels [8–12], FSW can be utilized to join different grades of the same material and dissimilar material combinations [13–16]. Researchers have, in the past,

experimented with FSW of different combinations of materials, such as aluminum alloys AA 7075-O and AA 5052-O [17], aluminum AA 3003 and AISI A441 steel [18], aluminum and stainless steel [19, 20], aluminum and brass [21], copper and brass [22], polymer PMMA [23], aluminum-magnesium alloy and polycarbonate [24], etc.

In FSW, the success of welding relies on the following: (i) heat generated by friction is sufficient enough to plasticize the material; (ii) proper mixing of the plasticized material; (iii) the size of the grains in the welded region. The welded joints are characterized by the output parameters such as tensile strength, elongation, and hardness,. To optimize the process parameters, the entire-process simulation of FSW based on experimental validation was adopted for the prediction of tensile strength. This simulation included the computational fluid dynamics (CFD) model and the computational solid mechanics (CSM) model [25, 26]. Huang et al. [27] proposed a fluid-solid interaction algorithm to establish the coupling model by treating the material to be welded as a non-Newtonian fluid. The high-throughput screening method, based on the fusion of parallel computational methods and an existing database containing calculated properties, is capable of exploring the hypothetical candidates [28], and the amelioration via the material flow model inhibits the welding defects and optimizes the parameter ranges, providing references to extract process-structure-property linkages for FSW. Ramesha et al. [17] performed dissimilar welding using different grades of aluminum alloy and observed that the higher rotational speed and medium speed of travel of the tool produce joints with higher hardness and tensile strength. In the case of welding dissimilar materials, the thickness of the intermetallic compound (IMC) layer formed affects the strength of the joint. The temper condition of the material to be welded also influences the joint quality. İpekoğlu et al. [8] investigated the joint quality of FSWed aluminum alloy with O and T6 temper conditions. The joints produced in the O temper condition exhibited comparably good strength, and lower strength was observed in the T6 temper condition when compared with the base metal. GürelÇam and GüvenİpekoğlustatedÇam found that the tensile strength and ductility of the welded joints are relatively low in the case of FSW of difficult-to-weld aluminum alloys. To overcome this problem to a certain extent, it is suggested to use external or in-process cooling [3]. Derazkola et al.[18] have used three different coolants, such as forced air, water, and CO_2, to investigate their effects on the joint strength. It was found that the metallurgical bonding, apart from the mechanical bonding due to the mixing of materials, due to the formation of an optimum layer of IMC when using a forced water-cooling medium, has increased the joint's strength in comparison with the other media. The grains are refined due to dynamic recrystallization by the adequate generation of heat at higher rotational speeds and a moderate feed rate [20].

Submerged FSW is a further advancement of FSW where the process is carried out under some medium such as water, and brine. The current authors of [29] have discussed in detail the advantages and limitations of submerged FSW over FSW in air from previous research. Aluminum alloy materials are very widely used in marine structures and the ship building industry due to their excellent corrosion-resistant properties. Several studies have been conducted on the underwater FSW of lightweight materials such as aluminum alloy [30], aluminum pipe [31], and magnesium alloy [32]. Aside from that, the welding of various materials, such as Al alloy and Mg alloy [33], Al and steel [34, 35], Al and stainless steel [36], and composite material [37], has been investigated under underwater conditions in the past.

In underwater FSW, an increase in the rotating speed of the tool and a decrease in welding speed significantly improved the mechanical properties of the joints, like in conventional FSW [38]. Kumar et al. [39] found that the order in which the process parameters affect the hardness of the underwater welded joints was rotational speed, traverse speed, and pin length. It was also observed that microcracks and porosity were present during dye penetrant tests in the UWFSW joints made at low speeds but were absent at higher speeds. Consequently, grain refinement is so significant in underwater FSW because of the faster cooling rate and lower peak temperature, and hence improved tensile strength and hardness are achieved [40–42]. Fine equiaxed grains are formed by the dynamic recrystallization caused by the heat generated, which significantly improves the mechanical properties of the welded joints [32]. Voids are observed in conventional FSW, and the size of the void formed and the fractional void area are reduced in UWFSW, also known as submerged friction stir welding (SFSW), which delays the cavity-induced fracture [43].

The maximum heat generated in the FSW of aluminum alloy is more than the UFSW, both in the experiment and simulation carried out by Khalaf et al. [44]. The higher heat generated in FSW results in enhanced material softening than in UFSW. The higher rate of cooling and controlled heat generation underwater conditions reduced the residual stress and strain. The authors have investigated the FSW of 1 mm thick titanium in both air and water and compared the tensile properties of the joints made at different process parameters [45, 46]. It was noticed that the yield strength and tensile strength of the SFSWed joints are much higher when compared with the FSW. The improvement in tensile properties of SFSW is due to the combined effects of proper stirring for thorough mixing and the hardening effect of the water environment. Warpage was observed after the welding in both FSW and SFSW because of the 1 mm thickness of the used sheet material. Higher torque and, hence, higher power consumption are the major limitations of the SFSW process [47]. Titanium and its alloys are difficult to plasticize sufficiently during FSW, and the nonuniform distribution of heat in the weld zone due to the poor thermal conductivity imposes a challenge [5]. From the review of the literature, it is observed that very few investigations are performed in FSW and SFSW using titanium, a lightweight material that is widely used at present. The aim of this paper is to evaluate the welded joints made by FSW and SFSW of a 2 mm-thick pure titanium sheet at different process parameters. For the evaluation, tensile property measurements, microstructural investigation, and nondestructive testing were performed.

The results of this research work help in establishing the proper process parameters to achieve the improved tensile properties of the welded joints in air and water.

2. Materials and Methods

The 2 mm-thick pure titanium plates with a size of 80×100 mm are used for experimental work. The chemical composition and the basic tensile properties of the base metal are shown in Tables 1 and 2. A custom-made setup to simulate the underwater environment was fabricated for performing the SFSW, while the conventional FSW was carried out by firmly clamping the workpieces directly on the machine table. No shielding gas was employed during the FSW process. The computer-numerically controlled vertical machining center (CNC) was used for the welding process both in air and water.

High carbon high chromium (HCHCr) steel was the cold-work tool steel material used for the tool in both FSW in air and water, and the hardness of the tool is maintained between 52 and 55 HRc. The details of the FSW tool are presented in Table 3.

The different process parameters used in the present experimentation for both welding in air and water are as follows: tool rotational speeds are 400 and 500 rpm, and tool travel speeds are 80–360 mm/min. The selection of the tool rotational speed for the current study was based on the previous work carried out by the authors [45, 46].

The tensile properties of the welded joints made in air and underwater were measured by conducting tests in a universal tensile testing machine according to ASTME-E8. The specimen for tensile testing was cut in a direction perpendicular to the welded direction, as shown in Figure 1. Three tensile specimens for each set of process parameters were tested, and the average value was computed. Images of the welded region were taken using an optical microscope and a scanning electron microscope (SEM) to investigate the microstructure formed during the welding process and compare it with the microstructure of the base metal. The Vickers microhardness was measured from the center of the weld at equidistance in the stir zone using a 300 g load for a dwell time of 10 sec. Nondestructive testing, such as radiography and dye penetrant tests, was carried out to detect the surface and interior defects in the welded joints.

3. Results and Discussion

Figures 2 and 3 display the welded sheets produced using different process parameters by the FSW and SFSW processes, respectively. From the visual inspection itself, it can be seen that the welding defects, such as incomplete filling, overburnt marks (which appear as black spots), and blow holes, are noticeable. The burnt effect during the welding process is due to the generation of excessive heat when the tool travelling speed is less than 140 mm/min at selected tool rotational speeds. While increasing the tool travelling speed beyond a certain value produced incomplete welding due to low heat generation and lower metal flow. The samples of the occurrence of such defects are displayed in Figure 4.

Table 1: Composition of base metal.

Elements	Fe	C	Ti
Observed weight (%)	0.022	0.001	99.87

Table 2: Basic tensile properties of base metal.

Test parameters	Observed values
Ultimate tensile strength (MPa)	349
Yield strength (MPa)	245
Elongation 50 GL (%)	34.5

Table 3: Details of FSW tool.

Descriptions	Details/values
Tool pin shape	Cylindrical
Pin diameter	10 mm
Pin length	1.8 mm
Shoulder diameter	14 mm
Overall diameter	16 mm
Overall length	115 mm

The HCHCr tool material used has high wear and abrasion resistance properties due to its higher % of chromium (approximately 12%). Also, since it was heat treated to 52–55 HRc, the tool wear is not noticeable.

3.1. Evaluation of Tensile Properties. Figures 5–7 exhibit the different tensile properties of the welded joints produced using different process parameters in air and underwater. The yield strength (YS) and tensile strength (TS) of the welded joint are decreased when the tool travelling speed is increased from 140 mm/min to 240 mm/min at both the tool rotational speeds of 400 and 500 rpm. A further increase in tool travelling speed to 400 rpm produced very weak welding. The value zero indicates that the welded joint was broken during handling or while clamping the specimen for tensile testing itself. However, at 500 rpm, the YS and TS of the welded joints are better than those obtained in the joints made at 400 rpm when the travelling speed is increased from 240 to 360 mm/min. It can be seen in FSW carried out in air that, at higher travelling speeds of 400 and 500 rpm, the heat generated is not sufficient to make a joint properly, and hence the tensile properties are lower, which extends to the level of breaking while handling itself, and also that the difference between the yield and tensile strengths is much lesser. The maximum measured YS and TS are 49.4% and 37.5% of the base metal, respectively, at the process parameters of 400 rpm and 140 mm/min. When the rotational speed is increased to 500 rpm, the maximum YS and TS observed are 59.2% and 46.1% of the base metal, respectively, at 140 mm/min welding speed. The improvement in the tensile properties at 500 rpm may be attributed to the reason that the increase in rotational speed generates more frictional heat, which is enough to plasticize the material, and the low traversing speed thoroughly mixes the flowing material to form a better joint. Very weak joints are formed at 400 and

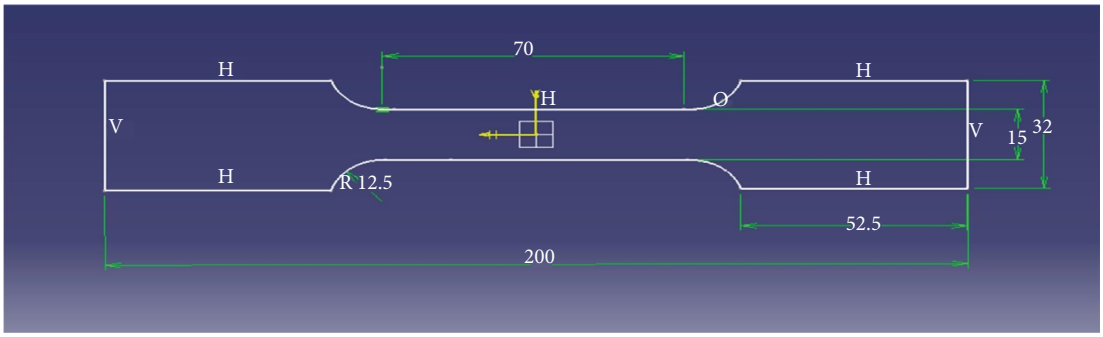

(a)

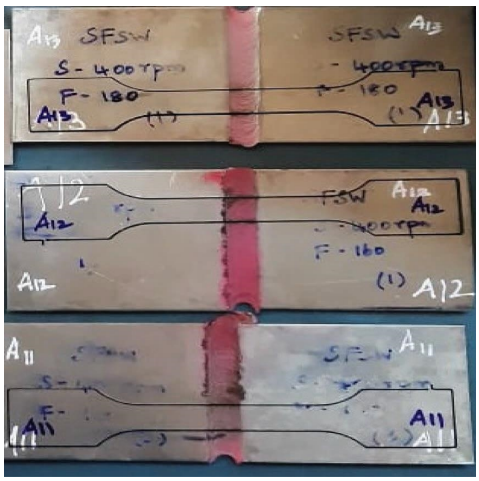

(b)

Figure 1: (a) Dimensions of the tensile specimen; (b) tensile specimens cut from the welded joints.

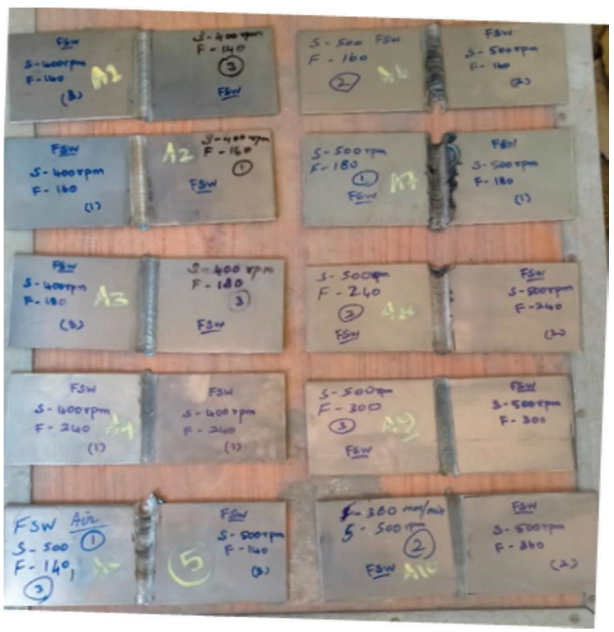

Figure 2: Friction stir welded joints at different process parameters.

Figure 3: Submerged friction stir welded joints at different process parameters.

Figure 4: Defects observed. (a) Burnt effect in air. (b) Burnt effect in water. (c) Incomplete filling in SFSW.

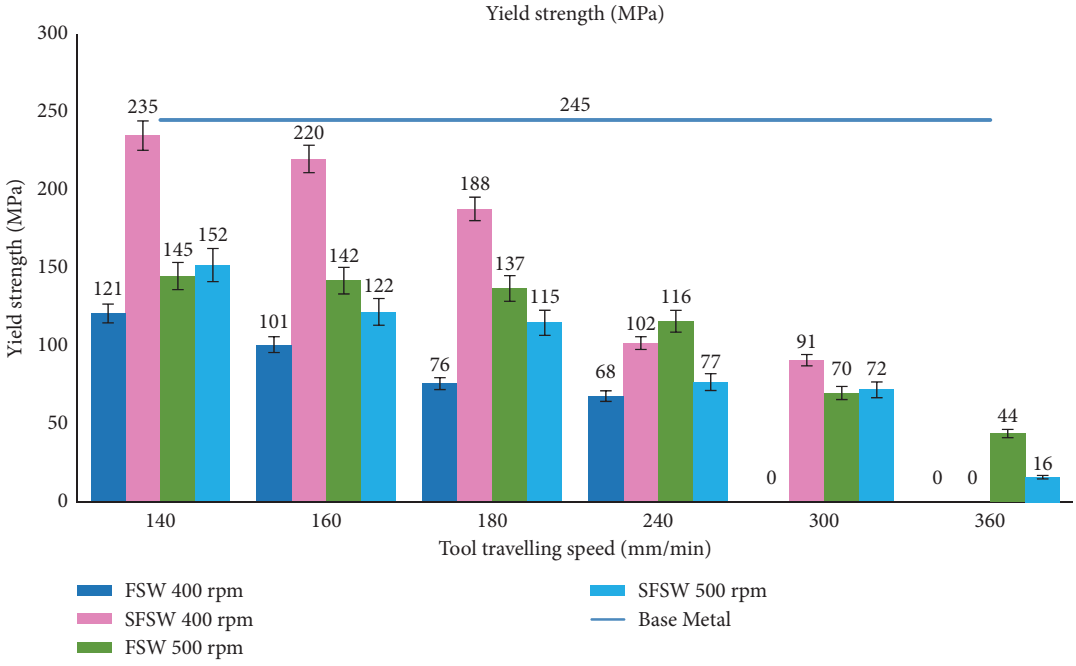

Figure 5: Yield strength of the welded joints.

500 rpm with the traversing speed above 240 mm/min due to the combined effects of improper material flow and insufficient heat generation.

In the case of underwater FSW, the YS and TS measured were maximum, which are 95.9% and 75.1% of the base metal values, respectively, when the tool rotational speed is 400 rpm and the travelling speed is 140 mm/min. These values are 94.2% and 100% higher than those obtained in conventional FSW, respectively, at the same process parameters. When the rotational speed is increased from 400 rpm to 500 rpm at a constant travelling speed of 140 mm/min, both YS and TS decrease. The same trend as that of conventional FSW was observed when the traversing speed was increased from 140 mm/min to UWFSW. The reason for an increase in YS and TS values in UWFSW when compared to FSW in air may be attributed to the reason that the heat generated is observed by the surrounding water and the faster cooling caused the hardening effect when the

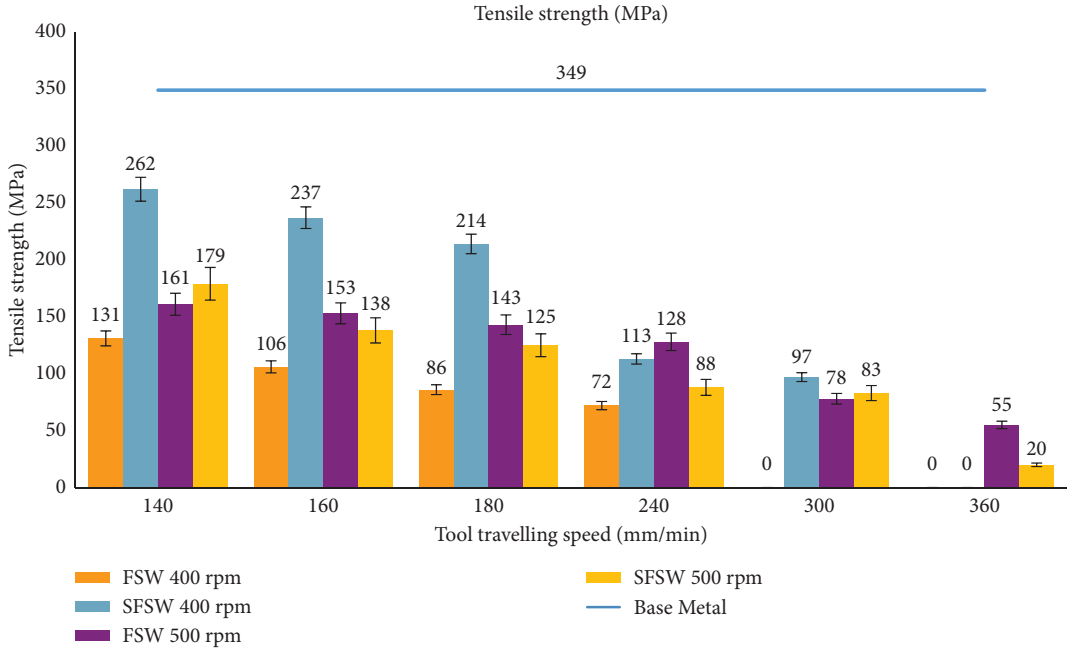

Figure 6: Tensile strength of the welded joints.

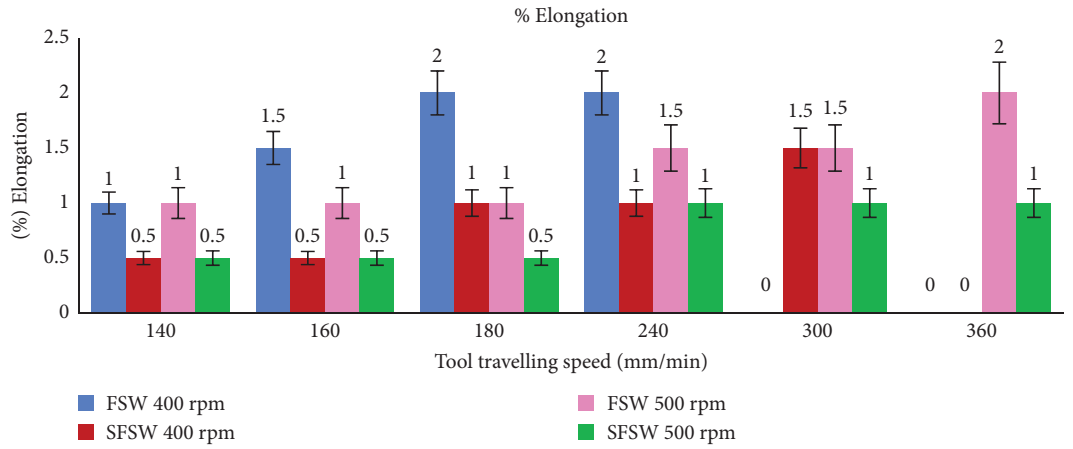

Figure 7: % Elongation of welded joints.

process parameters are at 400 rpm and 140 mm/min. The cooling rate is slower at 500 rpm than it is at 400 rpm at the same travelling speed, and hence, the YS and TS values at 500 rpm are lower than those that were observed at 400 rpm at the constant travelling speed.

The % elongation in FSW and UWFSW joints is much lower when compared with the values observed in base metal. The reason for this is confined plasticity in the weld region due to the presence of strength undermatching, which results in elongation only in the weld region of tensile specimens while the rest of the specimen is in an elastic regime during the test [48]. Higher strain concentration in the strength undermatching joints causes fracture at the lower strength weld region, and hence, the % elongation is lowered significantly [49]. Similar low elongation values were also reported for many fusion-weldedAl-alloys joints or other joints produced by of electron beam welding [50] and laser welding [51], with significant strength undermatching in the weld region [48]. Lower ductility was observed not only in different fusion welding processes but also in different materials and their combinations, such as dual-phase steel [11], brass [9], similar structural steel [12], and dissimilar structural steel [13]. Also, the % elongation in UWFSW is lower than that of FSW in air due to the hardening effect caused by the faster cooling rate of the surrounding water. Due to the improvement in the yield and tensile strength of the welded joints, the % elongation in SFSW carried out at a speed of 400 and 500 rpm when the travelling speed is at 140–160 mm/min is lower than the FSW. Furthermore, an increase in the travelling speed decreases the strength of the joints in both SFSW and FSW, thereby, increasing the % elongation.

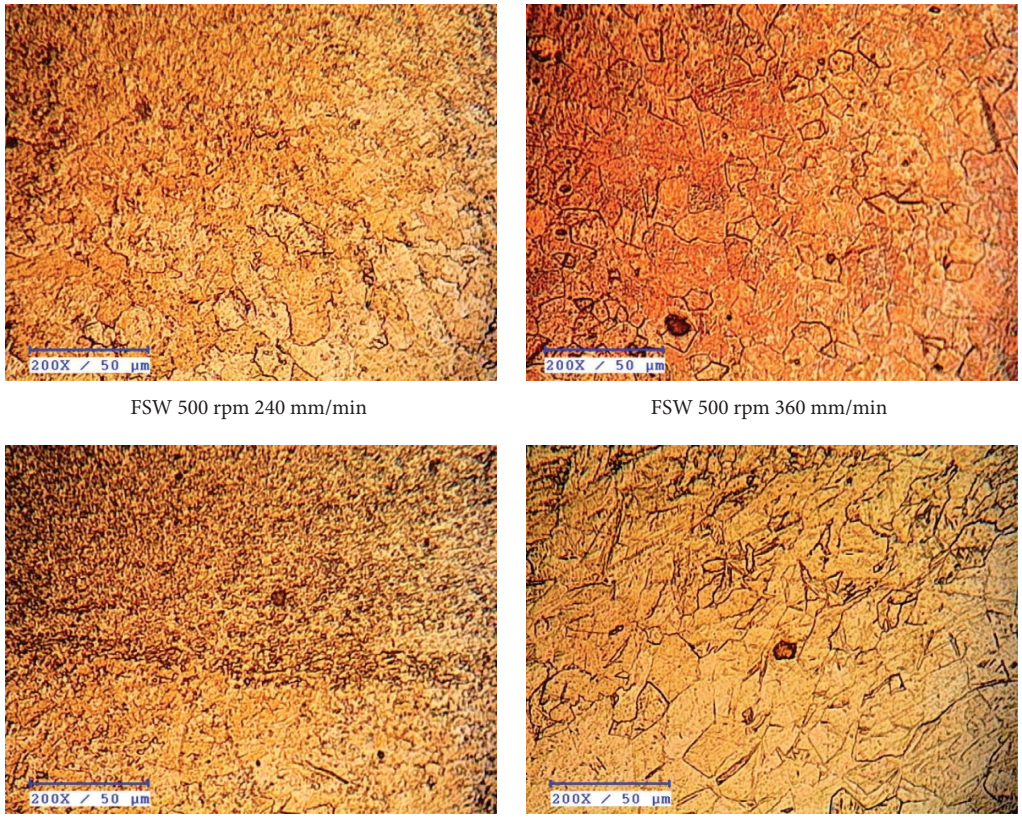

FSW 500 rpm 240 mm/min FSW 500 rpm 360 mm/min

SFSW 400 rpm 140 mm/min SFSW 500 rpm 240 mm/min

Figure 8: Optical microscopic images of the welded joints.

3.2. Evaluation of Microstructure. The sample optical microstructure images of the welded joints with improved and poor tensile properties made in FSW and SFSW are exhibited in Figure 8. The observed microstructure of the submerged friction-stir welded joint shows uniformly distributed, equiaxed finer grains than the conventional FSW joint grains, resulting in improved tensile properties in the underwater environment compared to that of the air environment. The size of the grains formed are depends on the combined effect of heat generated by friction, proper mixing of plasticized material, and the rate of cooling. A cooled underwater environment helps in the smooth flow of the plasticized material at optimum heat generated by the stirring tool, which causes a better recrystallization process at the stir zone. Furthermore, the presence of water helps in maintaining a uniform heat supply along the entire weld line. Due to these, the joints made by SFSW showed higher resistance to failure by fracture compared with conventional FSW. The sample scanning electron microscope (SEM) images of the welded joints made in air and water environment are shown in Figure 9. It is seen from the images that the flow of material is smooth at the lower travelling speed when the rotating speeds are maintained at 400 rpm and 500 rpm. The proper mixing of material along with the cooling effect improves the tensile properties of the joints made in an underwater environment. When the tool travelling speed is increased at the same rotational speed, there is incomplete mixing and small voids are formed, which reduces the tensile properties of the welded joints in both conventional and underwater FSW.

3.3. Evaluation of Microhardness. Figure 10 shows the distribution of microhardness in the stir zone of the welded joints made in FSW and SFSW. In general, the microhardness depends on the size of the material grains. A sufficient heat input increases the hardness when cooled faster, and drastic cooling by a water medium increases the hardness even when the heat input is higher. The restriction on grain growth caused by dynamic recrystallization during the higher cooling rate also increases microhardness. The refinement of the grain is related to the severe plastic deformation that is caused by the stirring action of the tool. At the optimum process parameters, the finer grains are formed, which account for the higher hardness of the joint made. Since the amount of heat generated depends on the rotational and travelling speeds of the tool and the rate of cooling, which depends on the working environment, the hardness of the welded joint is higher in UWFSW at 400 rpm and 140 mm/min than in FSW.

3.4. Evaluation of Defects by Nondestructive Testing. The sample results of the dye penetrant tests performed on the joints made by conventional and underwater FSW are presented in Figure 11. The dye penetrant test images showed

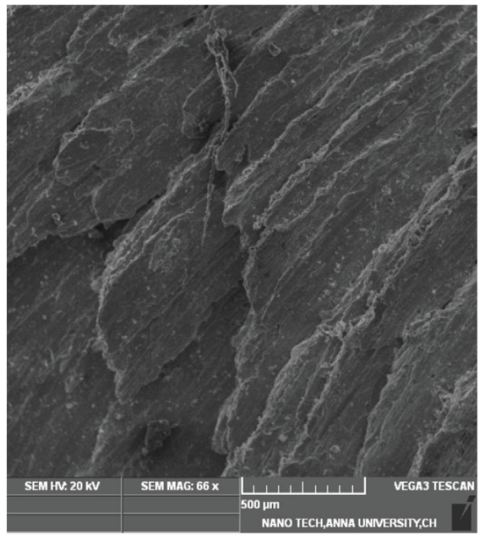

FSW 500 rpm 140 mm/min

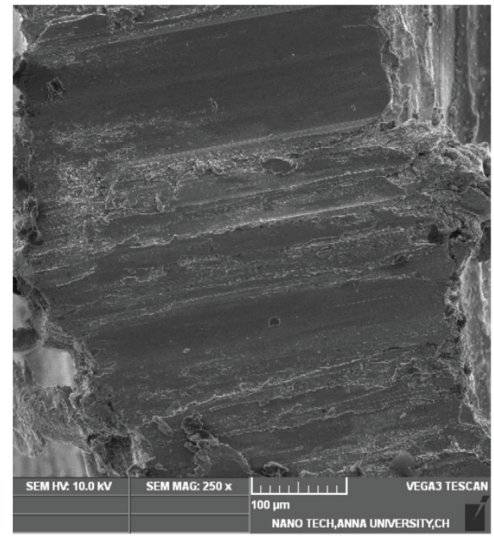

FSW 500 rpm 240 mm/min

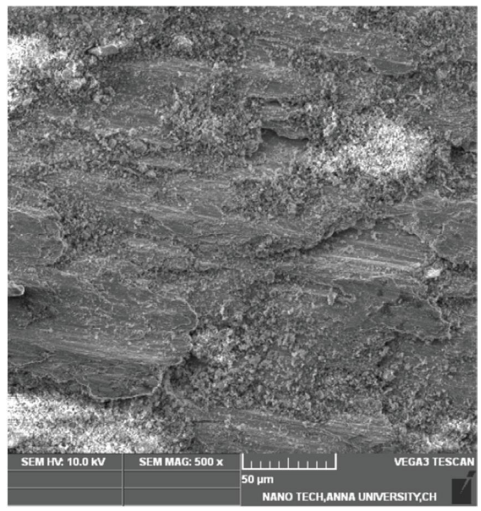

SFSW 400 rpm 140 mm/min

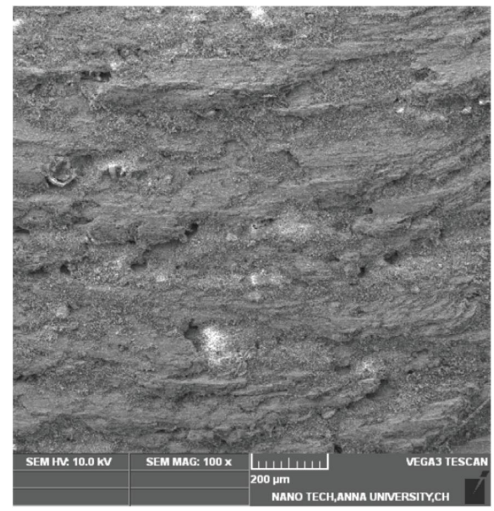

SFSW 500 rpm 300 mm/min

Figure 9: Scanning electron microscopic images of welded samples.

uniform waviness along the entire weld line, which indicates the proper flow of plasticized material in both types of the welding process. Also, no surface defects such as cracks, and dents. were observed in all joints made in air and water. The images of the welded joints taken with X-ray radiography are shown in Figure 12. The stir zone in the welded joint produced at 400 rpm and 180 mm/min in an air environment shows a perfect mixing of material without any internal defects. The incomplete joint formed at a higher travelling speed due to insufficient heat input and improper mixing of material is very clearly seen by the existence of a line, which indicates that the welding is not proper in the bottom region of the plates. A similar effect was observed in the welded joints made for the underwater environment, too.

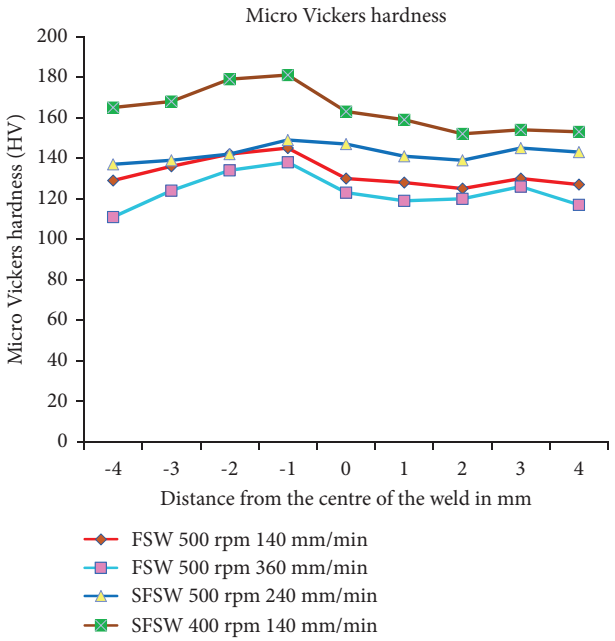

Figure 10: Micro-Vickers hardness of the welded joints.

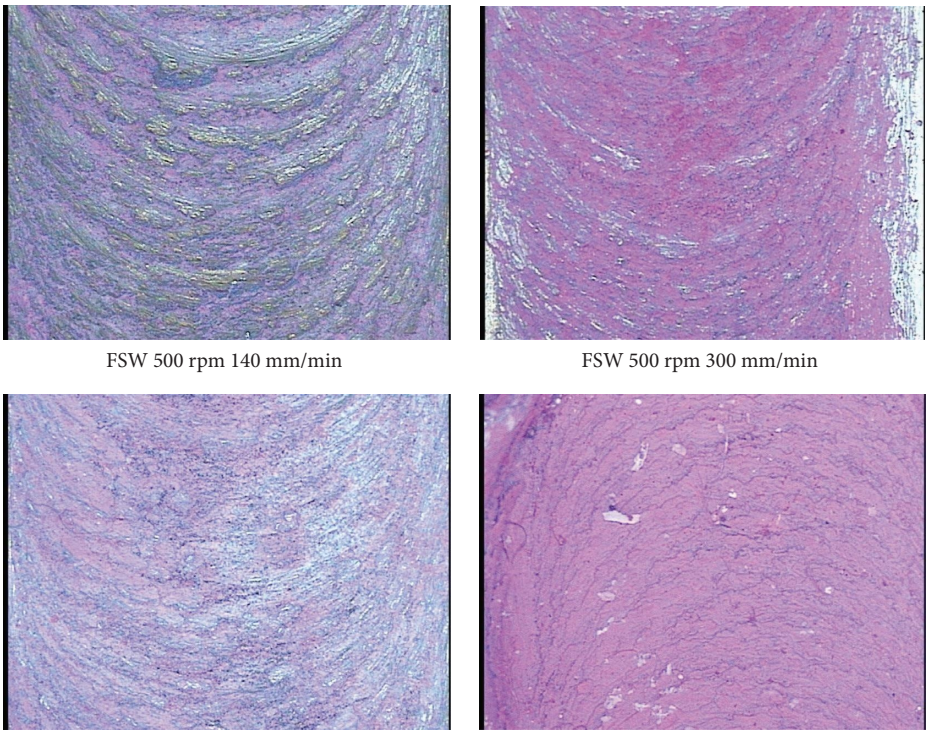

FSW 500 rpm 140 mm/min

FSW 500 rpm 300 mm/min

SFSW 400 rpm 140 mm/min

SFSW 400 rpm 240 mm/min

Figure 11: Dye penetrant test images of the welded joints.

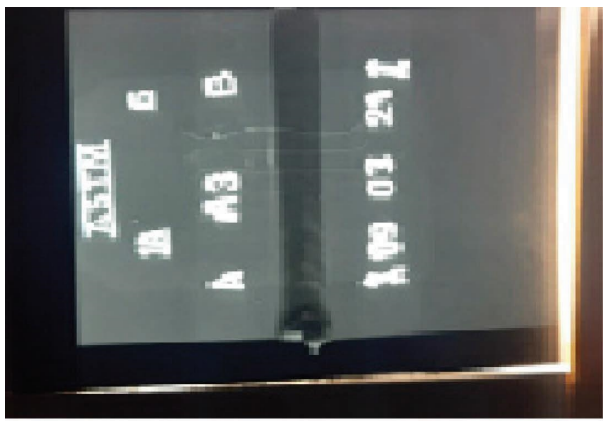

FSW 400 rpm180 mm/min (without defect)

FSW 500 rpm 300 mm/min (with defect)

SFSW 400 rpm 180 mm/min (without any internal defects)

SFSW 500 rpm 300 mm/min (with incomplete filling defect)

Figure 12: X-ray radiography images of the welded joints.

4. Conclusions

FSW was performed on a 2 mm-thick titanium sheet in both an air and water environment. The evaluation of the joints formed is performed by mechanical and microstructural analysis. The following conclusions are drawn from the results of the present research work:

(a) The maximum observed values of YS and TS in tensile testing are 49.4% and 37.5% of the base metal, respectively, at the process parameters of 400 rpm and 140 mm/min in conventional FSW. When the rotational speed is increased to 500 rpm and the welding speed remains the same, the maximum YS and TS observed are 59.2% and 46.1% of the base metal, respectively.

(b) In underwater FSW, the improved YS and TS values are observed, which are 95.9% and 75.1% of the base metal values, respectively, when the tool rotational speed is 400 rpm and the travelling speed is 140 mm/min. These values are 94.2% and 100% higher than those of the results obtained in conventional FSW at the same process parameters.

(c) The % elongation in both types of FSW joints is much lower than the base metal. The higher strain concentration in the strength undermatching joints (confined plasticity) is the reason for the lower % elongation. Also, due to the hardening effect caused by the faster cooling rate of the surrounding water, the % elongation in UWFSW is lower than that of FSW in air.

(d) Equiaxed finer grains are observed in the joint produced at 140 mm/min tool travelling speed in both the FSW in the air and underwater. The grains in the underwater FSW joints are finer than those of the conventional FSW.

(e) The images from optical microscopy and SEM support very well the results of the tensile testing. Small voids are clearly visible in the joints produced at higher welding speeds, which indicate improper mixing of material due to insufficient heat input.

(f) The microhardness value of the UWFSW joint is higher than the conventional FSW at a lower travelling speed of 140 mm/min, and an increase in the tool's travelling speed decreases the hardness in both FSW and UWFSW.

(g) No surface defects, such as cracks or pores, are observed from the results of the dye penetrant test in the successfully made joints of FSW and underwater FSW.

(h) Similarly, no internal defects are noticeable in X-ray radiography tests in the successfully made joints of FSW and underwater FSW. However, incomplete filling is observed in the joints made in both cases at higher tool travelling speeds.

Data Availability

All the data generated or analyzed during this study are available from the corresponding author upon reasonable request.

Disclosure

This research received no specific grant from any funding agency in the public, commercial, or not-for-profit sectors.

Conflicts of Interest

The authors declare that they have no conflicts of interest.

Acknowledgments

The authors thank the management of Dr. M.G.R. Educational and Research Institute for their continuous support and the encouragement.

References

[1] X. Meng, Y. Huang, J. Cao, J. Shen, and J. F. dos Santos, "Recent progress on control strategies for inherent issues in friction stir welding," *Progress in Materials Science*, vol. 115, Article ID 100706, 2021.

[2] N. Kashaev, V. Ventzke, and G. Çam, "Prospects of laser beam welding and friction stir welding processes for aluminum airframe structural applications," *Journal of Manufacturing Processes*, vol. 36, pp. 571–600, 2018.

[3] G. Çam and G. İpekoğlu, "Recent developments in joining of aluminum alloys," *International Journal of Advanced Manufacturing Technology*, vol. 91, no. 5, pp. 1851–1866, 2017.

[4] G. Çam, G. İpekoğlu, and H. TarıkSerindag, "Effects of use of higher strength interlayer and external cooling on properties of friction stir welded AA6061-T6 joints," *Science and Technology of Welding and Joining*, vol. 19, no. 8, pp. 715–720, 2014.

[5] G. Çam, "Friction stir welded structural materials:beyond Al-alloys," *International Materials Reviews*, vol. 56, no. 1, pp. 1–48, 2011.

[6] Y. Zhou, S. Chen, J. Wang, P. Wang, and J. Xia, "Influences of pin shape on a high rotation speed friction stir welding joint of a 6061-T6 aluminum alloy sheet," *Metals*, vol. 8, no. 12, p. 987, 2018.

[7] W. Boonchouytan, J. Chatthong, and P. Muangjunburee, "Microstructural and mechanical properties of welded SSM356-T6 and SSM7075-T6 aluminum semi-solid sheets by friction stir welding," *Engineering and Applied Science Research*, vol. 43, no. 4, pp. 189–195, 2016.

[8] G. İpekoğlu, S. Erim, B. G. Kiral, and G. Çam, "Investigation inti the effect of temper condition on friction stir weldability of AA6061 Al-alloy," *Metallic Materials*, vol. 51, no. 03, pp. 155–163, 2021.

[9] G. Çam, S. Mistikoglu, and M. Pakdil, "Microstructural and mechanical characterization of friction stir butt joint welded 63% Cu-37% Zn brass plate," *Welding Journal*, vol. 88, pp. 225–232, 2009.

[10] G. Çam, H. T. Serindağ, A. Cakan, S. Mistikoglu, and H. Yavuz, "The effect of weld parameters on friction stir welding of brass plates," *Materialwissenschaft und Werkstofftechnik*, vol. 39, no. 6, pp. 394–399, 2008.

[11] T. Küçükömeroğlu, S. M. Aktarer, and G. Çam, "Investigation of mechanical and microstructural properties offriction stir welded dual phase (DP) steel," *IOP Conference Series: Materials Science and Engineering*, vol. 629, no. 1, Article ID 012010, 2019.

[12] T. Küçükömeroğlu, S. M. Aktarer, G. İpekoğlu, and G. Çam, "Microstructure and mechanical properties of friction-stir welded St52 steel joints," *International Journal of Minerals, Metallurgy and Materials*, vol. 25, no. 12, pp. 1457–1464, 2018.

[13] T. Küçükömeroğlu, S. M. Aktarer, G. İpekoğlu, G. Çam, and G. Çam, "Mechanical properties of friction stir welded St 37 and St 44 steel joints," *Materials Testing*, vol. 60, no. 12, pp. 1163–1170, 2018.

[14] G. İpekoğlu, T. Küçükömero, S. M. Aktarer, D. M. Sekban, and G. Cam, "Investigation of microstructure and mechanical properties of friction stir welded dissimilar St37/St52 joints," *Materials Research Express*, vol. 6, no. 4, Article ID 046537, 2019.

[15] G. İpekoğlu and G. Çam, "Effects of initial temper condition and postweld heat treatment on the properties of dissimilar friction-stir-welded joints between AA7075 and AA6061 aluminum alloys," *Metallurgical and Materials Transactions A*, vol. 45, no. 7, pp. 3074–3087, 2014.

[16] G. Çam, V. Javaheri, and A. Heidarzadeh, "Advances in FSW and FSSW of dissimilar Al-alloy plates," *Journal of Adhesion Science and Technology*, pp. 1–33, 2022.

[17] K. Ramesha, P. D. Sudersanan, N. Santhosh, and S. Jangam, "Design and optimization of the process parameters for friction stir welding of dissimilar aluminium alloys," *Engineering and Applied Science Research*, vol. 48, no. 3, pp. 257–267, 2021.

[18] H. A. Derazkola, E. García, A. Eyvazian, and M. Aberoumand, "Effects of rapid cooling on properties of aluminum-steel friction stir welded joint," *Materials*, vol. 14, no. 4, p. 908, 2021.

[19] R. P. Mahto, S. Anishetty, A. Sarkar, O. Mypati, S. K. Pal, and J. D. Majumdar, "Interfacial microstructural and corrosion characterizations of friction stir welded aa6061-T6 and AISI304 materials," *Metals and Materials International*, vol. 25, no. 3, pp. 752–767, 2019.

[20] P. Goel, A. W. Mohd, N. Sharma, A. N. Siddiquee, and A. Zahid, "Effects of welding parameters in friction stir welding of stainless steel and aluminum," in *Advances in Industrial and Production Engineering*, K. Shanker, R. Shankar, and R. Sindhwani, Eds., pp. 815–823, Springer, Singapore, 2019.

[21] N. Osman, Z. Sajuri, and M. Z. Omar, "Multi-pass friction stirred clad welding of dissimilar joined AA6061 aluminium alloy and brass," *Journal of Mechanical Engineering and Sciences*, vol. 12, no. 4, pp. 4285–4299, 2018.

[22] F. Gharavi, I. Ebrahimzadeh, K. Amini, B. Sadeghi, and P. Dariya, "Effect of welding heat input on the microstructure and mechanical properties of dissimilar friction stir-welded copper/brass lap joint," *Materials Research*, vol. 22, no. 4, 2019.

[23] M. Elyasi and H. A. Derazkola, "Experimental and thermo-mechanical study on FSW of PMMA polymer T-joint,"

International Journal of Advanced Manufacturing Technology, vol. 97, no. 1-4, pp. 1445–1456, 2018.

[24] H. A. Derazkola and M. Elyasi, "The Influence of process parameters in friction stir welding of Al-Mg alloy and polycarbonate," *Journal of Manufacturing Processes*, vol. 35, pp. 88–98, 2018.

[25] Y. M. Xie, X. Meng, and Y. Huang, "Entire process simulation of friction stir welding —Part 1: experiments and simulation," *Welding Journal*, vol. 101, no. 5, pp. 144–159, 2022.

[26] Y. M. Xie, X. Meng, and Y. Huang, "Entire-process simulation of friction stir welding —Part 2: implementation of neural networks," *Welding Journal*, vol. 101, no. 6, pp. 172–177, 2022.

[27] Y. Huang, Y. Xie, X. Meng, J. Li, and Li Zhou, "Joint formation mechanism of high depth-to-width ratio friction stir welding," *Journal of Materials Science and Technology*, vol. 35, no. 7, pp. 1261–1269, 2019.

[28] Y. Huang, Y. Xie, X. Meng, Z. Lv, and J. Cao, "Numerical design of high depth-to-width ratio friction stir welding," *Journal of Materials Processing Technology*, vol. 252, pp. 233–241, 2018.

[29] N. Ethiraj, S. Meikeerthy, and T. Sivabalan, "Submerged friction stir welding: an overview of results of experiments and possible future works," *Engineering and Applied Science Research*, vol. 47, no. 1, pp. 111–116, 2020.

[30] F. Heirani, A. Abbasi, and M. Ardestani, "Effects of processing parameters on microstructure and mechanical behaviors of underwater friction stir welding of Al5083 alloy," *Journal of Manufacturing Processes*, vol. 25, pp. 77–84, 2017.

[31] I. Sabry and N. Zaafarani, "Dry and underwater friction stir welding of aa6061 pipes - a comparative study," *IOP Conference Series: Materials Science and Engineering*, vol. 1091, no. 1, Article ID 012032, 2021.

[32] W. Liu, Y. Shen, and C. Guo, "Microstructures and mechanical properties of submerged friction stir welding of ME20M Magnesium alloy," in *Proceedings of the 2019 16th International Bhurban Conference on Applied Sciences and Technology (IBCAST)*, pp. 1–6, IEEE, Islamabad, Pakistan, January, 2019.

[33] Y. Zhao, Z. Lu, K. Yan, and L. Huang, "Microstructural characterizations and mechanical properties in underwater friction stir welding of aluminum and magnesium dissimilar alloys," *Materials and Design*, vol. 65, pp. 675–681, 2015.

[34] A. Eyvazian, A. Hamouda, F. Tarlochan, H. A. Derazkola, and F. Khodabakhshi, "Simulation and experimental study of underwater dissimilar friction-stir welding between aluminium and steel," *Journal of Materials Research and Technology*, vol. 9, no. 3, pp. 3767–3781, 2020.

[35] H. A. Derazkola and F. Khodabakhshi, "Underwater submerged dissimilar friction-stir welding of AA5083 aluminum alloy and A441 AISI steel," *International Journal of Advanced Manufacturing Technology*, vol. 102, no. 9-12, pp. 4383–4395, 2019.

[36] R. P. Mahto, C. Gupta, M. Kinjawadekar, A. Meena, and S. K. Pal, "Weldability of AA6061-T6 and AISI 304 by underwater friction stir welding," *Journal of Manufacturing Processes*, vol. 38, pp. 370–386, 2019.

[37] X. Li, Z. Zhang, Y. Peng et al., "Microstructure and mechanical properties of underwater friction stir welding of CNT/Al-Cu-Mg composites," *Journal of Materials Research and Technology*, vol. 18, pp. 405–415, 2022.

[38] M. Hajinezhad and A. Azizi, "Numerical analysis of effect of coolant on the transient temperature in underwater friction stir welding of Al6061-T6," *International Journal of Advanced Manufacturing Technology*, vol. 83, no. 5-8, pp. 1241–1252, 2016.

[39] J. Kumar, S. Majumder, A. K. Mondal, and R. K. Verma, "Influence of rotation speed, transverse speed, and pin length during underwater friction stir welding (UW-FSW) on aluminum AA6063: a novel criterion for parametric control," *International Journal of Lightweight Materials and Manufacture*, vol. 5, no. 3, pp. 295–305, 2022.

[40] K. T. Babu, S. Muthukumaran, C. B. Kumar, and C. S. Narayanan, "A study on influence of underwater friction stir welding on microstructural, mechanical properties and formability in 5052-O aluminium alloys," *Materials Science Forum*, vol. 969, pp. 27–33, 2019.

[41] M. A. Wahid, Z. A. Khan, A. N. Siddiquee, R. Shandley, and N. Sharma, "Analysis of process parameters effects on underwater friction stir welding of aluminum alloy 6082-T6," *Proceedings of the Institution of Mechanical Engineers - Part B: Journal of Engineering Manufacture*, vol. 233, no. 6, pp. 1700–1710, 2019.

[42] M. A. Wahid, A. N. Siddiquee, Z. A. Khan, and N. Sharma, "Analysis of cooling media effects on microstructure and mechanical properties during FSW/UFSW of AA 6082-T6," *Materials Research Express*, vol. 5, no. 4, Article ID 046512, 2018.

[43] E. E. Kishta and B. Darras, "Experimental investigation of underwater friction-stir welding of 5083 marine-grade aluminum alloy," *Proceedings of the Institution of Mechanical Engineers - Part B: Journal of Engineering Manufacture*, vol. 230, no. 3, pp. 458–465, 2016.

[44] H. I. Khalaf, R. Al-Sabur, M. E. Abdullah, A. Kubit, and H. A. Derazkola, "Effects of underwater friction stir welding heat generation on residual stress of aa6068-T6 aluminum alloy," *Materials*, vol. 15, no. 6, p. 2223, 2022.

[45] S. Meikeerthy and N. Ethiraj, "Characterization of submerged friction stir welded joints of titanium," *Design Engineering*, vol. 5, pp. 2312–2325, 2021.

[46] E. Narasimhalu, S. Thanapal, V. Kumar Jayakumar et al., "Investigation on properties of the welded joints by friction stir welding of titanium under air and water," *Surnaree Journal of Science and Technology*, vol. 28, no. 6, Article ID 010086, 2021.

[47] C. Rathinasuriyan, S. Muniamuthu, A. Mystica, and V. S. Senthil Kumar, "Investigation of heat generation during submerged friction stir welding on 6061-T6 aluminum alloy," *Materials Today Proceedings*, vol. 46, pp. 8320–8324, 2021.

[48] G. Çam, V. Ventzke, J. F. Dos Santos, M. Koçak, G. Jennequin, and P. Gonthier-Maurin, "Characterisation of electron beam welded aluminium alloys," *Science and Technology of Welding and Joining*, vol. 4, no. 5, pp. 317–323, 1999.

[49] G. İpekoğlu and G. Çam, "Formation of weld defects in cold metal transfer arc welded 7075-T6 plates and its effect on joint performance," *IOP Conference Series: Materials Science and Engineering*, vol. 629, no. 1, Article ID 012007, 2019.

[50] G. Çam and M. Koçak, "Microstructural and mechanical characterization of electron beam welded Al-alloy 7020," *Journal of Materials Science*, vol. 42, no. 17, pp. 7154–7161, 2007.

[51] G. Çam, M. Koçak, and J. F. Dos Santos, "Developments in laser welding of metallic materials and characterization of the joints," *Welding in the World*, vol. 43, no. 2, 1999.